PERGAMON

International Journal of Heat and Mass Transfer 45 (2002) 1945–1949

International Journal of HEAT and MASS TRANSFER

www.elsevier.com/locate/ijhmt

A Monte Carlo model for predicting the effective emissivity of the silicon wafer in rapid thermal processing furnaces

Y.H. Zhou [a], Y.J. Shen [a], Z.M. Zhang [a,*], B.K. Tsai [b], D.P. DeWitt [b]

[a] *Department of Mechanical Engineering, University of Florida, Gainesville, FL 32611, USA*

[b] *Optical Technology Division, National Institute of Standards and Technology, Gaithersburg, MD 20899, USA*

Received 11 April 2001; received in revised form 28 August 2001

Abstract

Advances in microelectronics led to the development of rapid thermal processing (RTP). Accurate in situ temperature measurement and control are crucial for RTP furnaces to be largely accepted in the fabrication of semiconductor chips. This paper describes an effective emissivity model based on the Monte Carlo method to facilitate radiometric temperature measurements. The results showed that for non-diffuse wafers the "true" effective emissivity (defined in this paper) should be used, instead of the hemispherical effective emissivity, to correct thermometer readings. The geometric parameters and surface radiative properties can significantly influence the effective emissivity. The numerical aperture of the lightpipe radiation thermometer and the wafer-to-shield distance may be optimized to improve the measurement accuracy. Published by Elsevier Science Ltd.

1. Introduction

Rapid thermal processing (RTP) is a semiconductor manufacturing technique for single wafer processing and has been applied to silicon epitaxy, thermal oxidation, thermal annealing, and thin-film deposition [1]. Due to continuous advances in microelectronics technology, RTP has been gradually replacing batch furnace processing. RTP systems require real-time wafer temperature measurement because the wafer inside is never in thermal equilibrium with the heating source. Zhang [2] reviewed non-contact techniques for surface temperature measurements; lightpipe radiation thermometers (LPRTs) are frequently chosen to monitor the temperature of the wafer.

Fig. 1 shows a cylindrical enclosure model for the lower chamber of the RTP test bed at the National Institute of Standards and Technology (NIST) [3]. The silicon wafer is heated on the top by an array of quartz-halogen lamps. A highly reflective cold shield (a gold-coated plate attached on a water-cooled platform) is used to enhance the effective emissivity of the wafer. The guard tube and the guard ring are made up of quartz and coated with a platinum film to increase their reflectivity. A sapphire lightpipe, wrapped in a sheath, views a small portion (hereafter referred to as "spot") of the wafer through an opening at the center of the shield. In the shield, there are four off-center holes that can accommodate additional lightpipes. The wafer temperature T is related to the measured radiance temperature T_λ and the effective emissivity $\varepsilon_{\mathrm{eff}}$ by [4],

$$1/T = 1/T_\lambda + \lambda \ln(\varepsilon_{\mathrm{eff}})/c_2, \quad (1)$$

where $c_2 = 14\,388$ μm K is the second radiation constant and λ is the central wavelength of the narrow-band filter in the LPRT. The requirement for the temperature measurement uncertainty is ±2 °C (95% confidence level) at 1000 °C, as specified in the International Technology Roadmap for Semiconductors (ITRS-2000). Accordingly, the relative uncertainty of the (spectral) effective emissivity must be less than ±2% for $\lambda \approx 1$ μm.

The net-radiation method was used to predict the hemispherical effective emissivity [5]. The algorithm is fast and convenient. However, if two or more surfaces are non-diffuse, the specular view factor is difficult to

* Corresponding author.
E-mail address: zmzhang@ufl.edu (Z.M. Zhang).

0017-9310/02/$ - see front matter. Published by Elsevier Science Ltd.
PII: S0017-9310(01)00295-2

Nomenclature

d	displacement in the z-direction
h	height on the guard tube
L	distance between the wafer and the shield
N	number of bundle rays
NA	numerical aperture of the lightpipe
r	radius
T, T_λ	wafer temperature and radiance temperature
W	energy per bundle

Greek symbols

α, θ, and φ	circumferential, polar, and azimuthal angles
ε	(spectral) emissivity
θ_h	half angle of the acceptance cone
λ	wavelength

Subscripts

e,s	ending and starting
eff	effective
lp, sh, and w	lightpipe, shield, and wafer
sp	(view) spot on the wafer

obtain. In addition, the strong temperature non-uniformity and the large property variation and roughness on the surfaces in an RTP furnace may cause significant angular dependence of the effective emissivity. The LPRT views the wafer through only a small acceptance cone with a half angle θ_h, which is often characterized by the numerical aperture $\mathrm{NA} = \sin\theta_h$. A more complicated statistical approach, i.e., the Monte Carlo method, is the preferred choice to study the angular dependence. Monte Carlo methods have been applied to predict the effective emissivity of nearly isothermal cavities [6,7]. Adams et al. [8] used a Monte Carlo model to predict the effective emissivity of the wafer in an RTP chamber. Their model, however, did not consider the effect of the guard ring and could not handle off-center LPRTs.

In the present work, a comprehensive Monte Carlo model is developed to study the lower chamber of RTP systems [9]. The influences of the wafer emissivity and specularity, the wafer-to-shield distance, and the numerical aperture on the effective emissivity are examined. The method presented here is not only applicable to an axisymmetric chamber, where the lightpipe is located at the center of the shield, but also to off-center LPRTs.

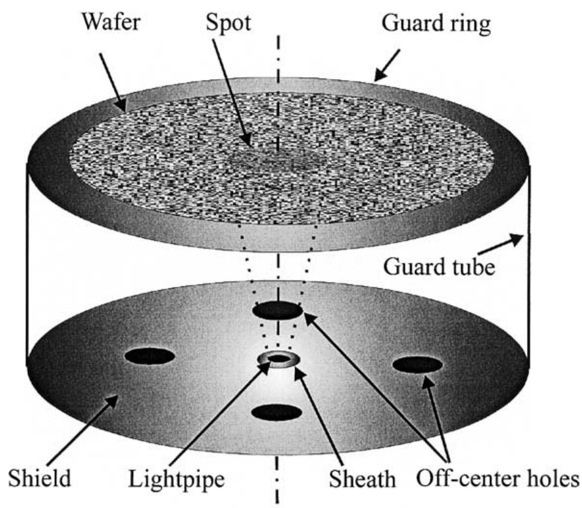

Fig. 1. Schematic of the lower chamber model for RTP furnaces (not to scale).

2. The Monte Carlo model

In this Monte Carlo model, all surfaces are assumed opaque and diffusely emitting. The wafer, the guard ring, and the shield are further divided into smaller concentric rings. On each ring, the properties and temperature are assumed uniform with extra consideration to the ring that contains the four off-center holes on the shield. In order to account for the roughness, the simple model in which the reflectivity is assumed to be composed of a specular component and a diffuse component is adopted here. The number of bundles emitted from the spot, denoted by N_{sp}, is chosen from a convergence analysis. The energy per bundle is calculated by $W = \varepsilon_w A_{sp} E_{\lambda,b}/N_{sp}$, where ε_w is the spectral emissivity of the wafer, A_{sp} is the area of the spot, and $E_{\lambda,b}$ is the blackbody emissive power. Different W may be used for different surface elements to reduce computational time because bundles from outer rings are less probable to reach the spot and then the lightpipe [8].

Four random numbers between 0 and 1 are generated to determine the position and direction for each bundle. The position is defined by a radius r on the top and bottom surfaces (or a height h on the guard tube) and a circumferential angle α. The direction of each bundle ray is defined by a polar angle θ and an azimuthal angle φ with respect to the surface normal. After the bundle ray is emitted, it will be traced in the enclosure until absorbed. For rays emitted or reflected from the top or bottom surfaces at a starting point (r_s, α_s) in the direction (θ, φ), the following equations determine the ending point (r_e, α_e) on the opposite surface:

$$r_e \cos\alpha_e = L\tan\theta\cos\varphi + r_s\cos\alpha_s,$$
$$r_e \sin\alpha_e = L\tan\theta\sin\varphi + r_s\sin\alpha_s. \tag{2}$$

When the calculated r_e is greater than r_{sh} (the radius of the shield), the ray will end up on the guard tube. For rays starting from the guard tube, the ending point is determined by:

$$r_e \cos\alpha_e = r_{sh}\cos\alpha_s + d(\sin\alpha_s\cos\varphi - \cos\alpha_s/\tan\theta)/\sin\varphi,$$
$$r_e \sin\alpha_e = r_{sh}\sin\alpha_s - d(\cos\alpha_s\cos\varphi + \sin\alpha_s/\tan\theta)/\sin\varphi, \tag{3}$$

where $d = h_e - h_s$ is the vertical displacement of the ray. One more random number is needed to determine whether the bundle is absorbed or reflected.

The local (hemispherical) effective emissivity of the wafer is calculated by

$$\varepsilon_{eff,w} = (N_{emitted,w} + N_{reflected,w})/N_{emitted,b}. \tag{4}$$

The numerator is the sum of emitted and reflected bundles from a surface element of the wafer, and the denominator is the number of bundles that would be emitted by a blackbody at the same temperature. Because only the bundles reaching the lightpipe from the spot contribute to the thermometer reading, a "true" effective emissivity is defined here for use to correct the LPRT reading:

$$\varepsilon_{eff,sp\text{-}lp} = N_{sp\text{-}lp}/N_{sp\text{-}lp,b}. \tag{5}$$

Here, the numerator is the number of bundles (emitted and reflected) from the spot to the lightpipe tip, and the denominator is the number of bundles from the spot to the tip if the spot were a blackbody. Because the lightpipe collects radiation within a certain numerical aperture, the effective emissivity may also be defined based on rays reaching the tip within θ_h, that is,

$$\varepsilon_{eff,\theta_h} = N_{within\,\theta_h}/N_{within\,\theta_h,b}. \tag{6}$$

Eq. (6) gives the hemispherical effective emissivity when $\theta_h = 90°$ and "true" effective emissivity when the actual numerical aperture is used. Eqs. (5) and (6) can be extended to determine the effective emissivity for off-center LPRTs, which are important for multi-point temperature measurements and control.

For the RTP system studied here, the radius of the wafer is 100 mm and the inner radius of the guard tube and the shield is 135 mm. The radii of the sapphire lightpipe, r_{lp}, and the sheath, r_{sh}, are approximately 1 and 2 mm, respectively. The off-center holes are located at 54 mm from the center of the shield with a radius of 3.5 mm. The adjustable distance between the wafer and the shield, L, is typically 12.5 mm. The radius of the spot is experimentally determined to be $r_{lp} + L/3$. In the simulation, a representative wafer temperature of 800 °C is chosen, and all other surfaces are set to be at 25 °C. The operating wavelength of the LPRT is 0.955 μm. At this wavelength, the radiation from all other surfaces is negligible compared with that from the wafer given their large temperature difference. The emissivity of a lightly doped silicon wafer varies from 0.68 at room temperature to 0.64 at 1000 °C. The reflectivity of the shield is 0.993. The emissivity of the guard ring and the guard tube is 0.1. The emissivities of the lightpipe, the sheath, and off-center holes are assumed to be the same as that of sapphire, which is 0.925. All surfaces in the lower chamber except the wafer are smooth and should reflect specularly.

Careful tests have been performed to check the random number generation scheme and the ray-tracing algorithm. A large number of random numbers are required, especially because the lightpipe tip is very small as compared with the chamber diameter. The choice of an appropriate algorithm for the random number generation is very important; an improved linear congruential generator, i.e., the shuffling algorithm due to Bays and Durham, is adopted here [10]. The computed view factor between the spot and the lightpipe tip converges within 0.5% after 3 million bundles. The absorption process can be checked using two infinite parallel plates. The probability for a bundle emitted from surface 1 (with an emissivity ε_1) to be absorbed at last by surface 1 after m bounces (round trip) is given by $p(m) = (1-\varepsilon_2)^m(1-\varepsilon_1)^{m-1}\varepsilon_1$, where ε_2 is the emissivity of the opposite surface. For typical emissivity values, the simulation results for both diffuse and specular plates agree within a relative error of 0.5% of the theoretical values calculated from the above equation after 0.1 million bundles are emitted from the spot. On the average, it takes less than 2 bounces before a bundle is absorbed for wafer emissivity greater than 0.5 (assuming that the shield is highly reflecting). Another ray-tracing method is to use the bundle energy partitioning, in which the unabsorbed bundle energy is traced until it is less than a certain portion, say 0.5% of the initial bundle energy. It will require more than 7 bounces for wafer emissivity of 0.5. Therefore, the method of bundle energy partitioning is less efficient for the present case because a large number of bundles are still required to obtain the correct directional distribution.

A reverse method is often used in optical design to greatly reduce the computational time. In this method, all the energy bundles are originated from the lightpipe tip to the wafer. However, the directional distribution of the bundles striking the lightpipe is complex and unknown [8]. In addition, the reverse method cannot handle the case when the wafer temperature is not uniform. Hence, only the forward method is presented in the following.

It takes about 4 million bundles from the spot for the $\varepsilon_{eff,sp\text{-}lp}$ to converge within ±0.005. The total number of emitted bundles is 1.5 billion and the computation takes about 11 h for each run on a 933 MHz Pentium III

personal computer. Under the thermal equilibrium condition (i.e., all surfaces at the same temperature), the Monte Carlo simulation predicts a hemispherical ε_{eff} of 1 ± 0.001 and a true ε_{eff} of 1 ± 0.004. The Monte Carlo simulation and the net-radiation method agree within 0.001 when all surfaces are diffuse without the off-center holes.

3. Results and discussion

Because the wafer emissivity may vary from batch to batch or during the processing due to the varied doping or coating materials and their thickness, it is important to know the influence of the wafer emissivity on the effective emissivity. Fig. 2 shows the true ε_{eff} and the hemispherical ε_{eff} as functions of ε_w. In this section, all surfaces are assumed specular unless indicated otherwise. The effective emissivity when all surfaces are diffuse is also plotted in Fig. 2. The error bar indicates an uncertainty of ± 0.005 (95% confidence) for $\varepsilon_{eff,sp\text{-}lp}$. The uncertainty for $\varepsilon_{eff,w}$ is less than 0.001. As ε_w is changed from 0.3 to 0.8, the $\varepsilon_{eff,sp\text{-}lp}$ increases from 0.945 to 0.990, whereas $\varepsilon_{eff,w}$ varies from 0.853 to 0.987. This suggests that the true ε_{eff} is less sensitive to the wafer emissivity variation, a desired feature for the radiometric temperature measurement. For $\varepsilon_w \leqslant 0.5$, the difference between $\varepsilon_{eff,sp\text{-}lp}$ and $\varepsilon_{eff,w}$ can be significant. The use of $\varepsilon_{eff,w}$ to obtain the wafer temperature will result in an error of about 1.7 °C in the temperature measurement. The experimental ε_{eff} obtained by comparison between a LPRT and thin-film thermocouples is approximately 0.98, which is close to the predicted values.

The effective emissivity calculated from Eq. (6) versus the numerical aperture of the lightpipe is shown in Fig. 3. The actual half angle of the lightpipe viewing the spot from the lightpipe center is 22.6° (NA = 0.384). The resulting $\varepsilon_{eff,\theta_h}$ is very close to that calculated from Eq. (5). As NA increases, $\varepsilon_{eff,\theta_h}$ increases first and then decreases, suggesting that the incoming intensity is not directionally uniform. There is little or no enhancement in the near-normal direction ($\theta_h \to 0$). The cold guard ring and guard tube contribute to the decrease in $\varepsilon_{eff,\theta_h}$ at large angles. For given wafer emissivity, there exists some optimized numerical aperture where $\varepsilon_{eff,\theta_h}$ becomes maximum. The half angle θ_h corresponding to the maximum $\varepsilon_{eff,\theta_h}$ is near 27° (NA = 0.45) for $\varepsilon_w = 0.3$. For higher wafer emissivities, there exists a plateau with higher $\varepsilon_{eff,\theta_h}$ values for $0.4 \leqslant \text{NA} \leqslant 0.8$. Hence, a choice of the half angle range from 24° to 30° (NA from 0.4 to 0.5) is recommended.

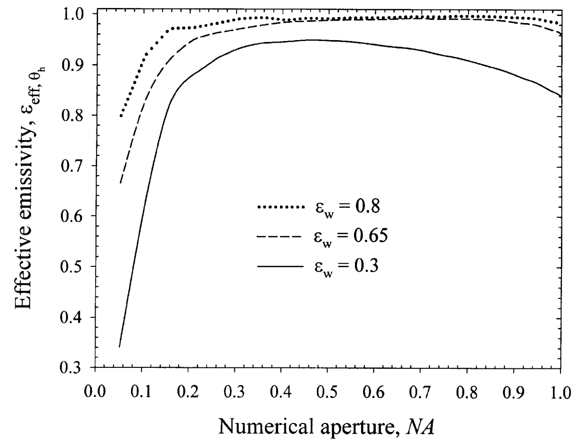

Fig. 3. The effective emissivity $\varepsilon_{eff,\theta_h}$ calculated from Eq. (6) vs. the numerical aperture.

The effect of the wafer-to-shield distance is demonstrated in Fig. 4 when $\varepsilon_w = 0.65$. The effective emissivity should be close to ε_w when L approaches zero. This has

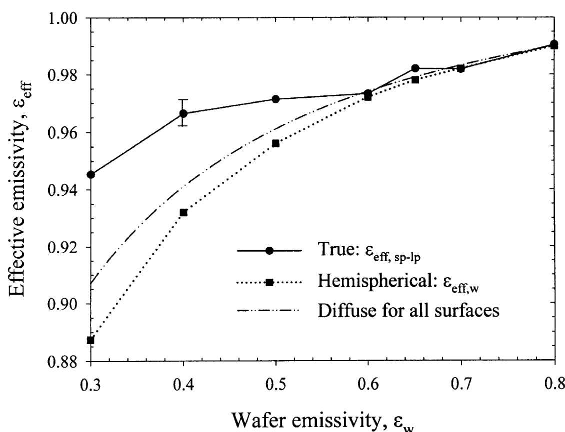

Fig. 2. The relationship between the effective emissivity and wafer emissivity.

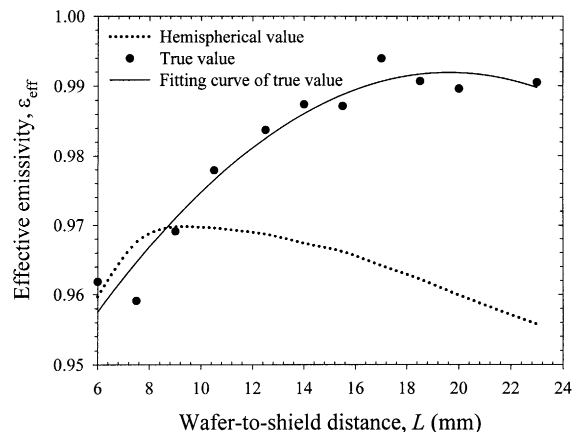

Fig. 4. The effective emissivity vs. the wafer-to-shield distance. The smooth curve is a quadratic fit from a regression analysis.

been verified from both the net-radiation and the Monte Carlo methods. As L increases, ε_{eff} increases first and then decreases when the influence of the cold guard ring and guard tube becomes important. As shown in Fig. 4, the value of L that maximizes $\varepsilon_{eff,w}$ is about 9 mm, which is very different from the one (about 20 mm) that maximizes the true ε_{eff}. At $L = 20$ mm, the true ε_{eff} assumes the maximum value of 0.99 which is 0.03 greater than the maximum $\varepsilon_{eff,w}$.

4. Conclusions

A Monte Carlo model has been developed to analyze the radiative transfer in the lower chamber of RTP furnaces. It can also be used to predict the effective emissivity for off-center LPRTs. The computational program developed here is generic and can be applied to model different RTP chamber geometries and surface radiative properties. For non-diffuse wafers, the "true" effective emissivity may deviate from the corresponding hemispherical value due to the angular dependence of the incoming radiation on the lightpipe. The deviation is even greater for specular wafers with an emissivity less than 0.5. The appropriate selection of the wafer-to-shield distance is important to maximize the true effective emissivity. For the conditions studied here, a numerical aperture of 0.4–0.5 (i.e., half angle of 24–30°) is recommended. In the future, the BRDF will be implemented in the numerical algorithm and the computational results will be compared with experimental data.

Acknowledgements

This work was supported by the National Science Foundation (CTS-9875441) and the NIST Office of Microelectronics Program. Jorge Garcia is acknowledged for his careful review of this manuscript.

References

[1] P.J. Timans, Rapid thermal processing technology for the 21st century, Mater. Sci. Semicond. Process. 1 (1998) 169–179.

[2] Z.M. Zhang, Surface temperature measurement using optical techniques, in: C.L. Tien (Ed.), Annual Review of Heat Transfer, vol. 11, Begell House, New York, 2000, pp. 351–411.

[3] C.W. Meyer, D.W. Allen, D.P. DeWitt, K.G. Kreider, F.L. Lovas, B.K. Tsai, ITS-90 calibration of radiometers using wire/thin-film thermocouples in the NIST RTP tool: experimental procedures and results, in: Proceedings of the 7th International Conference on Advances in Thermal Processing of Semiconductor, 1999, pp. 136–141.

[4] D.P. DeWitt, F.Y. Sorrell, J.K. Elliott, Temperature measurement issues in rapid thermal processing, Mater. Res. Soc. Symp. Proc. 470 (1997) 3–15.

[5] Z.M. Zhang, Y.H. Zhou, An effective emissivity model for rapid thermal processing using the net-radiation method, Int. J. Thermophys. 22 (2001) 1563–1575.

[6] Z. Chu, J. Dai, R.E. Bedford, Monte Carlo solution for the directional effective emissivity of a cylindro-inner cone, in: J.F. Schooley (Ed.), Temperature, Its Measurement and Control in Science and Industry, vol. 6, AIP, New York, 1992, pp. 907–912.

[7] V.I. Sapritsky, A.V. Prokhorov, Calculation of the effective emissivities of specular-diffuse cavities by the Monte Carlo method, Metrologia 29 (1992) 9–14.

[8] B. Adams, A. Hunter, M. Yam, B. Peuse, Determining the uncertainty of wafer temperature measurements induced by variations in the optical properties of common semiconductor materials, in: Proceedings of the 197th ECS Meeting, 2000, pp. 363–374.

[9] Y.H. Zhou, Y.J. Shen, Z.M. Zhang, B.K. Tsai, D.P. DeWitt, Impact of directional properties on the radiometric temperature measurement in rapid thermal processing, in: Proceedings of the 8th International Conference on Advances in Thermal Processing of Semiconductor, 2000, pp. 94–103.

[10] W.H. Press, S.A. Teukolsky, W.T. Vetterling, B.P. Flannery, Numerical Recipes in Fortran, second ed., Cambridge University Press, Cambridge, UK, 1992 (Chapter 2).